Neuroscience Letters 584 (2015) 362–367

Contents lists available at ScienceDirect

Neuroscience Letters

journal homepage: www.elsevier.com/locate/neulet

Short communication

Intranasal deferoxamine engages multiple pathways to decrease memory loss in the APP/PS1 model of amyloid accumulation

Jared M. Fine*, Daniel B. Renner, Anna C. Forsberg, Rachel A. Cameron, Benjamin T. Galick, Clint Le, Patrick M. Conway, Benjamin M. Stroebel, William H. Frey II, Leah R. Hanson

Health Partners Institute for Education and Research, Center for Memory and Aging, Regions Hospital, 640 Jackson St., Saint Paul, MN, USA

HIGHLIGHTS

- Intranasal DFO reduces working and reference memory loss in an amyloid mouse model.
- Intranasal DFO modifies several targets along multiple pathways in Alzheimer's.
- Intranasally administered DFO has potential for treatment of Alzheimer's disease.

ARTICLE INFO

Article history:
Received 1 July 2014
Received in revised form 3 November 2014
Accepted 7 November 2014
Available online 13 November 2014

Keywords:
Alzheimer's disease
Glycogen synthase kinase
Radial arm water maze
Malondialdehyde
Oxidative stress
Intranasal

ABSTRACT

In addition to the hallmark accumulation of amyloid and hyper-phosphorylation of tau, brain changes in Alzheimer's disease are multifactorial including inflammation, oxidative stress, and metal dysregulation. Metal chelators have been explored as a less well known approach to treatment. One chelator currently being developed is deferoxamine (DFO), administered via the intranasal (IN) route. In the current study, APP/PS1 amyloid mice were treated with a chronic, low dose of IN DFO, subjected to a rigorous battery of behavior tests, and the mechanism of action was examined. Mice were treated 3x/week with 0.24 C IN DFO for 18 weeks from 36 to 54 weeks of age, 4 weeks of behavior tests were performed that included both working and reference memory, anxiolytic and motor behaviors, and finally brain tissues were analyzed for amyloid, protein oxidation, and other proteins affected by DFO. We found that IN DFO treatment significantly decreased loss of both reference and working memory in the Morris and radial arm water mazes ($p < 0.05$), and also decreased soluble Aβ40 and Aβ42 in cortex and hippocampus ($p < 0.05$). Further, IN DFO decreased activity of GSK3β, and led to decreases in oxidative stress ($p < 0.05$). These data demonstrate that low doses of IN DFO can modify several targets along the multiple pathways implicated in the neuropathology of Alzheimer's, making it an attractive candidate for the treatment of this heterogeneous disease.

1. Introduction

Alzheimer's disease involves multifactorial brain changes including problems with amyloid and tau processing, neuronal degeneration, insulin dysregulation, synaptic loss, chronic inflammation, oxidative stress, and accumulation of metals [1–3]. The disruption of metal homeostasis has led to the suggested use of metal-binding agents as a potential therapeutic strategy [3]. Metal-binding agents currently being developed for the treatment of AD include clioquinol, PBT2, M30, and deferoxamine [4]. Deferoxamine (DFO) is an iron chelator that is FDA-approved for treatment of iron overload. Intraperitoneal injections of DFO in aged rats decreased age-related memory impairment and reduced oxidative damage [5], and an early clinical trial using intramuscular DFO in AD patients showed a 50% reduction in the rate of functional decline over a period of 2 years [6]. However, further development of DFO for the treatment of AD was complicated by limited blood–brain barrier permeability and side effects from systemic delivery. Delivering DFO via the intranasal route is an alternative to avoid these problems.

Abbreviations: AD, Alzheimer's disease; DFO, deferoxamine; Aβ, amyloid beta; IN, intranasal; GSK, glycogen synthase kinase; HIF, hypoxia inducible factor; PD, Parkinson's disease; RAWM, radial arm water maze; MWM, morris water maze; GFAP, glial fibrillary acidic protein; MDA, malondialdehyde; ROS, reactive oxygen species.

* Corresponding author. Tel.: +1 651 254 5101; fax: +1 651 254 3661.
E-mail address: jared.m.fine@healthpartners.com (J.M. Fine).

http://dx.doi.org/10.1016/j.neulet.2014.11.013
0304-3940/

Intranasal (IN) delivery is a non-invasive method of targeting drugs directly from the nose to the brain, and allows for DFO to be delivered with minimal systemic exposure. Intranasal delivery of DFO has been shown to have benefit in several animal models of Alzheimer's and Parkinson's disease [7–10]. Hanson et al. [8] showed a behavioral benefit of IN DFO in an amyloid mouse model, though it did not address any biochemical mechanisms, and behavioral analysis was limited to a single memory task. In the present study, APP/PS1 mice received long-term intranasal treatment with a 1% solution of DFO (0.24 mg/dose; 1/10th the dose in Hanson et al. [8]), were subjected to a rigorous battery of behavior tests (adapted from Arendash et al. [11]), and tissue samples were analyzed extensively for amyloid and other proteins related to DFO. We found that IN DFO significantly decreased memory loss in both working and reference memory, decreased soluble amyloid, and decreased protein oxidation in the brain. These data demonstrate the therapeutic efficacy of intranasally delivered DFO as a treatment for Alzheimer's disease, and show multiple targets in the disease process in which DFO can yield beneficial effects.

2. Methods

2.1. Animal care and treatment

A total of 51 male mice were purchased from Jackson laboratories (Bar Harbor, ME). Transgenic (TG) mice (34) were B6C3-Tg (APPswe, PSEN1dE9) 85Dbo/J (stock #004462), while 17 wild-type (WT) controls from the same background were acquired. Mice were acquired at 6 weeks of age, and had continuous access to food and water during a 12 h light/dark cycle. Mice were initially housed together, but eventually housed individually to prevent fighting. All procedures were approved by the Animal Care and Use Committee of Health Partners Institute for Education and Research at Regions Hospital under protocol #08-024.

2.2. Experimental design

Mice were divided into three treatment groups of 17 each: (1) TG mice given IN DFO (TG-DFO), (2) TG mice given IN phosphate buffered saline (TG-PBS), and (3) WT mice given IN PBS (WT-PBS). At 30 weeks of age, mice were acclimated to handling and then treated intranasally every monday, wednesday, and friday, starting at 36 weeks of age. Mice were dosed for 18 weeks, until behavior tests at 54 weeks. Dosing continued during the 4 weeks of behavior to measure both chronic and acute effects. After behavior mice were dosed a final time, and 24 h later euthanized and tissues collected for biochemical analyses. These included soluble and insoluble amyloid as measured by ELISA and IHC, quantification of proteins with Western blot and oxidative markers.

2.3. Drug treatment and dosing

Deferoxamine mesylate was purchased from Sigma (D9533; St. Louis, MO), and delivered as a 1% solution in 0.2x phosphate buffered saline (PBS; Sigma; P5493) at a pH of 6.0. The vehicle consisted of 0.2x PBS. For IN delivery, unanesthetized mice were given 24 μl (0.24 mg DFO) as in Hanson et al. [12].

2.4. Behavioral assessment

Mice were subjected to a battery of behavior tests to determine cognitive, anxiolytic, and sensorimotor functions over 4 weeks. To assess working memory, radial arm water maze (RAWM) was performed as in Fine et al. [7], except there were 4 trials/day, tests proceeded for 9 days, and a penalty was assessed for non-compliance. Specifically, if a mouse had three or less errors and 60 s escape latency, it was assessed a penalty of eight errors. The 9 days of data were divided into three blocks of 3 days. For reference memory, Morris water maze (MWM) was performed as in Fine et al. [7], except that hidden platform tests consisted of 5 successive days at one block of 4 trials/day. The elevated plus maze, open field, and rotarod were all performed exactly as in Fine et al. [7].

2.5. Euthanasia and tissue collection

Mice were anesthetized with a cocktail of ketamine, xylazine, and acepromazine and euthanized via transcardial perfusion with saline and protease inhibitors (Roche, Boulder, CO). Cortex and hippocampus were removed and snap-frozen in liquid nitrogen, with the exception of five mice from each group. These were processed for immunofluorescent analysis via cardiac perfusion with buffered 4% paraformaldehyde, paraffin embedding, and tissue sectioning.

2.6. Immunohistochemistry

For plaque load, four sagittal sections spaced 100 μm apart, located between 1–1.5 mM lateral of the mid-sagittal plane were stained from each mouse. Sections were probed with a 1:150 dilution of anti-amyloid 4G8 primary antibody (Sig-39220, Covance, NJ), followed by secondary staining with 1:200 dilution of Alexa Fluor 647 goat anti-mouse antibody (A-21235, Invitrogen, NY). Sections were counter-stained with DAPI. Z-Stack images of cortex and hippocampus were collected on an Olympus FluoView FV1000 IX2 inverted confocal fluorescent microscope at 100X. Image J software was used to define, count, and determine plaques in a defined region of interest. Imaging analysis was conducted by a blinded researcher.

2.7. Western blot analysis

Tissue was homogenized in RIPA buffer (50 mM Tris–HCl, pH 7.4, 150 mM NaCl, 2 mM EDTA, 1% sodium deoxycholate, 1% NP-40, 0.1% SDS) supplemented with protease inhibitor cocktail (Roche, Boulder, CO), and phosphatase inhibitor cocktail (Sigma, St. Louis, MO) and centrifuged at 20,000 × *g* for 20 min. Equal amounts of total protein (50 μg) were separated by SDS-PAGE, transferred to nitrocellulose and blotted with the following: phospho-GSK-3β (Ser9) rabbit antibody (#9323, Cell Signaling Technology, Beverly, MA), GSK-3β (27C10) mouse monoclonal antibody (#9832, Cell Signaling Tech.), HIF-1α rabbit polyclonal antibody (NB100-479, Novus Biologicals, Littleton, CO), β-catenin E-5 (sc-7963, Santa Cruz Biotechnology, Santa Cruz, CA). Staining for actin was used as a loading control (NB600-532, Novus Biologicals). The membranes were incubated with fluorescently labeled antibodies: IRDye 800CW Goat anti-rabbit (926-3221) and IRDye 650 goat anti-mouse (926-68020) (LiCor Lincoln, NE). Data was collected and analyzed with the odyssey imaging system (LiCor). Protein oxidation was measured using the oxyblot protein oxidation detection kit (S1750; Millipore, MA).

2.8. Amyloid ELISA and malondialdehyde assay

Soluble and insoluble Aβ40 and Aβ42 were measured in brain using commercially available ELISA kits (KHB3442 and KHB3482; Life Technologies, NY). For ELISA of soluble amyloid, frozen tissue was homogenized in extraction buffer (20 mM Tris, pH 7.4, 137 mM NaCl with protease inhibitor cocktail) and spun at 100,000 × *g* for 1 h. Insoluble amyloid was extracted from the pellet with homogenization in guanidine extraction buffer (50 mM Tris, pH 8.0, 5 M guanidine HCl) followed with centrifugation at 14,000 × *g* for 20 min. Oxidative stress was assessed colorimetrically by

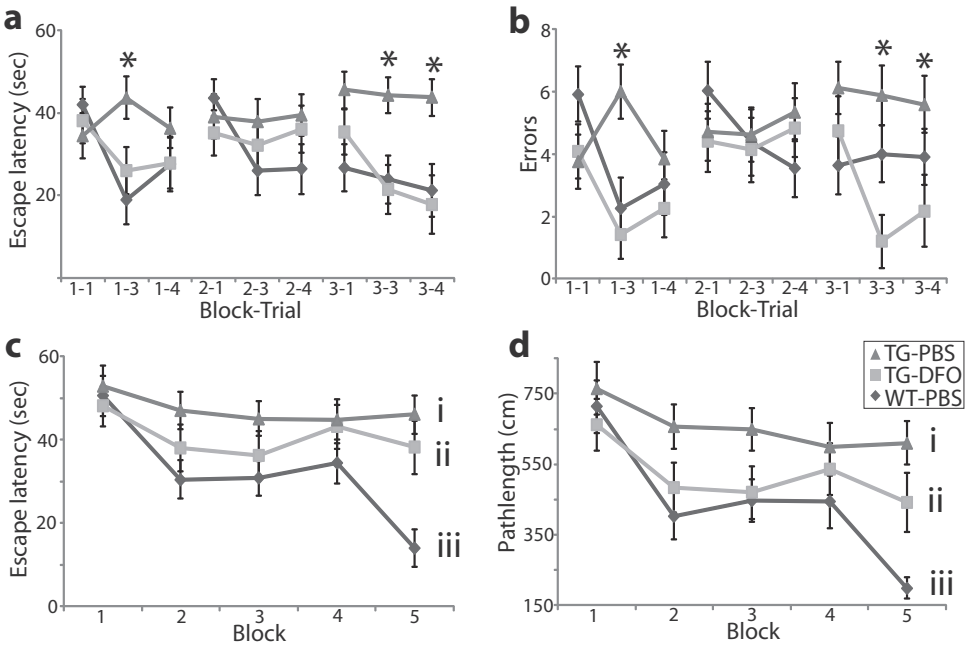

Fig. 1. Radial arm water maze (RAWM) and Morris water maze (MWM) data. APP/PS1 mice and WT-controls were treated 3x/weeks with IN DFO or PBS. In RAWM, 9 successive days were broken into 3 blocks of days 1–3, 4–6, and 7–9. Trials 1, 3, and 4 are shown. For both escape latency (a) and errors (b), WT-PBS and TG-DFO mice had significantly shorter escape time and fewer errors than TG-PBS mice in several trials as measured by ANOVA (*$p < 0.05$). For MWM, there were 5 successive days of four trials. The escape latency (c) and path-length (d) were averaged for trial 4, and repeated measures ANOVA showed each group to be significantly different from other groups (i–iii; $p < 0.05$).

measuring malondialdehyde (MDA) in brain tissue using a lipid peroxidation assay kit (ab118970; Abcam, MA).

2.9. Statistical analyses

Behavioral tests included parametric and non-parametric analyses. Non-parametric analyses were used for tests that included a truncation effect which violated assumptions of normality that included MWM visual platform, rotarod, and RAWM escape. For comparisons of three treatment groups, ANOVA with Fisher's LSD post-test (parametric) or Kruskal–Wallis with Dunn's post-test (non-parametric) was used. Repeated measures ANOVA was used for hidden platform tests in MWM. For all biochemical tests, *T*-tests or ANOVAs were used to compare treatment groups.

3. Results

3.1. General health

During the course of the study, six mice died of natural causes before the appointed sacrifice time at 58 weeks; three were WT-PBS, two were TG-DFO, and one was TG-PBS. There were no significant differences in weight of each treatment group ($p > 0.05$). Average weight (±SEM) was 45.53 ± 0.8 g for WT-PBS, 46.12 ± 1.2 g for TG-DFO, and 45.38 ± 1.0 g for TG-PBS. No obvious physical defects were observed.

3.2. Behavior

In the RAWM, TG-DFO mice had shorter escape latencies and fewer errors than TG-PBS mice in trials three and four for all blocks ($p < 0.05$; Fig. 1a and b). These differences were significant in trial three of block one, and trials three and four of block three ($p < 0.05$) using ANOVA. Wild-type mice also had significantly shorter escape latencies than TG-PBS mice in these trials ($p < 0.05$). For hidden platform tests in MWM, repeated measures ANOVA yielded a significant difference between all three treatment groups for both escape latency and path-length ($p < 0.05$; F:10.9, df:2; F:13.1, df:2; Fig. 1c and d). The shortest escape latency and path-length were for wild-type mice, while the longest were for PBS-treated TG mice. There were no significant differences among any groups in the visual platform MWM, elevated plus maze, open field or rotarod (data not shown).

3.3. Amyloid

Amyloid was not detectable in WT mice. For the five mice whose brains were for IHC (Fig. 2a), staining in the cortex and hippocampus demonstrated a trend towards decreased plaques in the cortex ($p = 0.07$), but differences were not significant (Fig. 2b). ELISA analyses demonstrated a decrease in both soluble and insoluble Aβ40 and Aβ42 for DFO-treated TG mice compared to PBS-treated TG mice (Fig. 2c). These decrease were significant for soluble Aβ40, in which DFO led to a 58% reduction ($p < 0.05$), and soluble Aβ42, in which DFO led to a 38.4% reduction ($p < 0.05$).

3.4. GSK pathway

Both pGSK3β and β-catenin were significantly increased by approximately 50% in the DFO-treated mice as compared to the untreated TG mice and WT controls ($p < 0.05$; F:6.5, df:2; F:5.3, df:2; Fig. 3a and b). As expected, there was no significant change in GSK3β itself (Fig. 3c), but there was for the ratio of pGSK3β/total GSK3β between the TG groups ($p < 0.05$; F:4.4, df:2; Fig. 3d).

3.5. Protein oxidation

Malondialdehyde levels in brain tissue were significantly decreased in DFO-treated mice as compared to both PBS-treated TG and WT mice ($p < 0.05$; F:3.8, df:2; Fig. 3e). There was also a trend toward a decrease in carbonyls in oxyblot for DFO-treated mice,

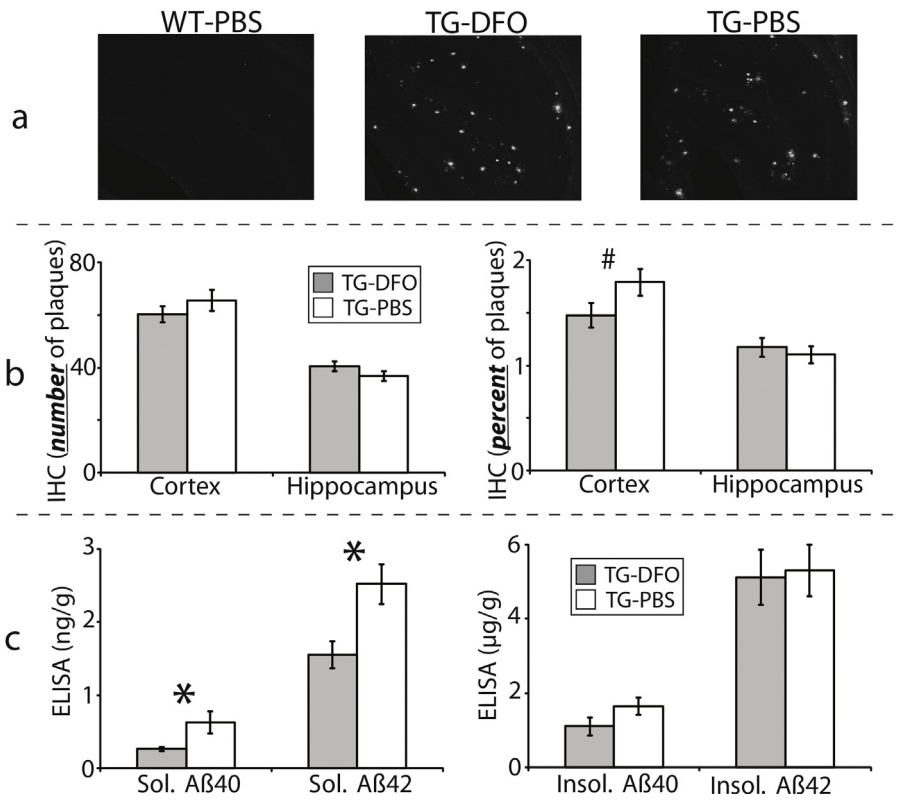

Fig. 2. Amyloid beta in brain tissue. TG mice are APP/PS1 dosed with IN DFO or PBS for 22 weeks. Representative slices from hippocampus from each of three treatment groups (a). For number and percent of plaques in the cortex and hippocampus (b), the only difference was a non-significant trend for fewer percent plaques in the cortex of DFO-treated mice ($p < 0.1$). As measured by ELISA (c), TG-DFO mice had significantly less soluble Aβ40 and Aβ42, but not significantly less insoluble amyloid. $^{*}p < 0.05$. $^{\#}p < 0.1$.

though not significantly despite the large percent change ($p = 0.07$) (Fig. 3f).

3.6. Additional analyses

There was no change in HIF-1α in any treatment groups (Fig. 3g). Glial fibrillary acidic protein (GFAP), the main astrocytic intermediate filament and marker for astrocyte activation, has been measured at increased levels in Alzheimer's patients and in transgenic amyloid mouse models [13]. In our study, western blots showed increased levels of GFAP in the TG model compared to WT mice ($p < 0.05$; F:5.0, df:2), but no effect was observed from DFO treatment (Fig. 3h). As measured by western blot, there was not a significant change in synaptophysin in cortex/hippocampus (Fig. 3i).

4. Discussion

Treatment of APP/PS1 mice with a chronic low dose of IN DFO decreased memory loss, soluble Aβ40 and Aβ42, protein oxidation, and GSK activity, demonstrating a benefit in this amyloid accumulation model via several modalities. This study utilizes a lower dose of DFO and a more complete battery of behavioral tests than previous studies, and attempts to address the question of mechanism of action. Intranasal DFO was safe and well-tolerated as evidenced by no change in weights or long term survival. The changes in soluble amyloid as well as oxidation suggest that DFO may be affecting the amyloid cascade. DFO has also been shown to be beneficial in the P301L tau model of AD, and protective effects were measured via pGSK, inflammation and oxidation, though no changes in tau were measured [7]. Because IN DFO is beneficial in several models of AD, and in other neurodegenerative diseases, it suggests DFO engages multiple targets to elicit a pleiotropic protective response in the brain.

In this study, IN DFO slowed the loss of memory in the APP/PS1 mouse model. A similar effect was seen in Hanson et al. [8]; however, in the current study mice were subjected to a full array of behavioral tests [11]. These tests included the Morris and radial arm water mazes to quantify both reference and working memory, as well as several other tests designed to measure anxiolytic and sensorimotor functions. This is important not only because DFO decreases memory loss at the 10x lower concentration, but it also paints a more complete picture of how the DFO is affecting the mice. Only the cognitive tests, not the anxiolytic or sensorimotor tests, showed any differences among groups, suggesting that DFO did not have any detrimental behavioral side-effects.

Mice treated with IN DFO had increased levels of pGSK3β and β-catenin, suggesting that the modification of GSK3 may be part of the mechanism for prevention of memory loss in this model. To our knowledge, this is the first demonstration of down-regulation of the GSK3 pathway in APP/PS1 mice. The GSK hypothesis of AD states GSK activity plays an important role in hyper-phosphorylation of tau, memory impairment, Aβ production, inflammatory responses, cholinergic deficit, and apoptosis [14]. Indeed, a number of these processes were affected by IN DFO treatment in this study, supporting the idea that DFO may be beneficial as a GSK inhibitor. Specifically, IN DFO increased phosphorylation of GSK at Ser9, decreasing GSK activity and increasing β-catenin. This increase in pGSK3β and β-catenin was seen in a tau mouse model in Fine et al. [7], though the increase in β-catenin in that study was not significant. This may be related to the 10x dose difference (2.4 mg DFO vs 0.24 mg DFO), or to the time difference between last dose and euthanasia, which was 30 min in Fine et al. [7], and 24 h in the current study. The regulation of GSK is not only relevant to AD, but a

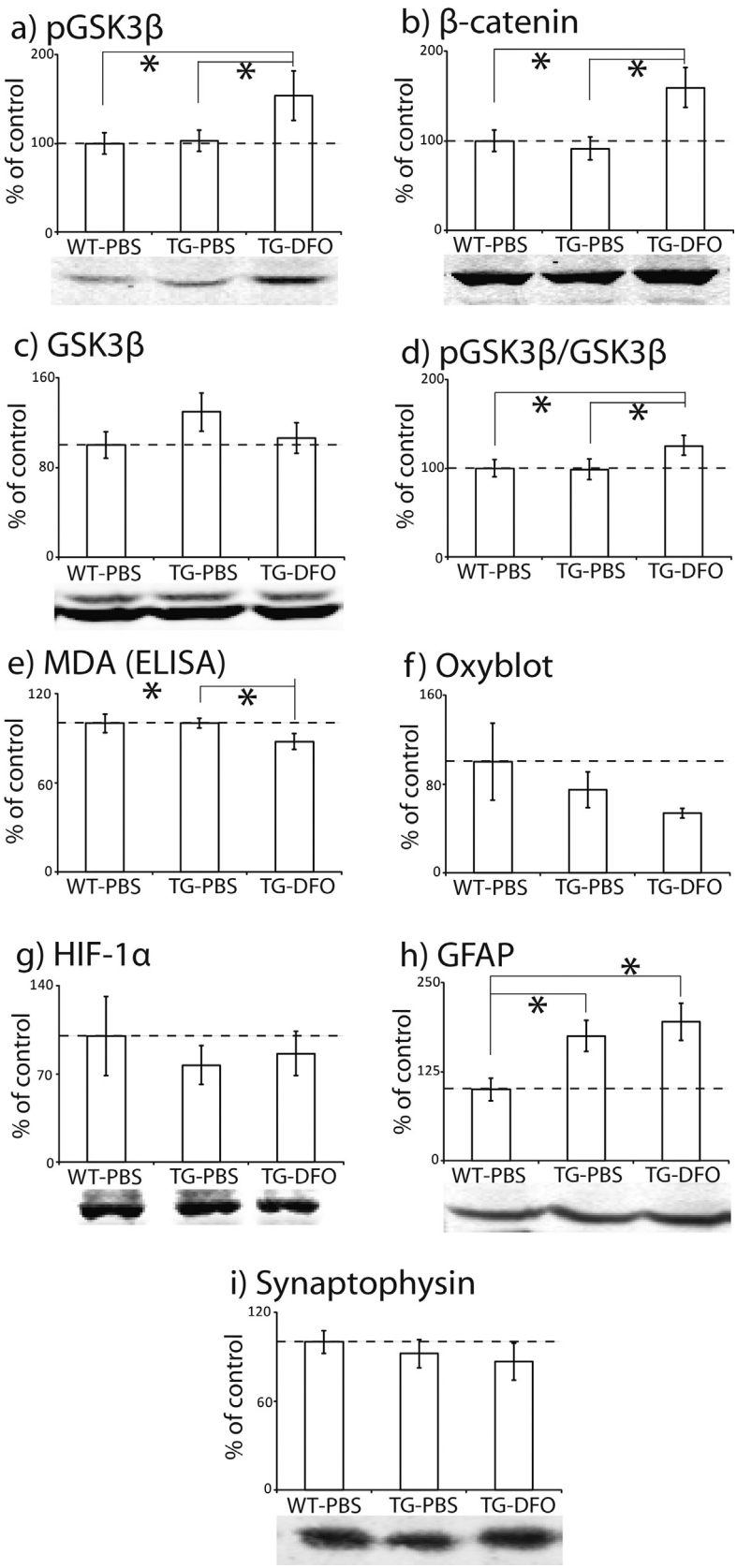

Fig. 3. Histograms for proteins analyzed by western blot, oxyblot, and an MDA kit. TG mice are APP/PS1 dosed with IN DFO or PBS for 22 weeks. (a) pGSK3β, (b) β-catenin, (c) GSK3β, (d) pGSK3β/GSK3β, (e) malondialdehyde, (f) oxyblot, (g) HIF-1α, (h) GFAP, and (i) synaptophysin. Bars in histograms are percent change from WT-PBS mice, which are given a default 100% and shown in each histogram by a dotted line. Error bars are SEM converted from the raw data to percentages and are only shown to help visualize differences. Statistical significance between groups as measured by ANOVA with Fisher's LSD post-test are represented with an asterisk ($^*p < 0.05$), and were performed on the raw data as optical density, not from percent changes.

number of neurodegenerative diseases [15]. Thus, it makes sense that IN DFO may be functioning as a GSK inhibitor in the AD model, as DFO has been found to be protective in several other neurodegenerative diseases including stroke, Parkinson's, Huntington's and TBI [16], and psychiatric disorders such as schizophrenia [17].

Intranasal treatment with DFO decreased oxidative stress, which occurs in AD [18]. The DFO-treated mice had lower levels of malondialdehyde, which is commonly used as a biomarker for lipid peroxidation as it is generated from reactive oxygen species (ROS) [19]. A decrease in malondialdehyde in response to DFO was seen in animal models of cerebral ischemia [20], spinal cord injury [21], and chronic stress [22], however, none of these studies utilized IN delivery. DFO-treated mice also had decreased levels of oxidation as measured by oxyblot. Though this decrease was large, it did not reach statistical significance ($p = 0.07$), likely due to high variation in the WT mice which affected the strength of ANOVA. One likely mechanism by which DFO would decrease oxidative damage is an increase in glycolysis and the associated hexose-monophosphate shunt from the stabilization of HIF-1α [23]. DFO stabilizes HIF-1α in in vitro studies, and did so in vivo when intranasally delivered to a tau mouse model in Fine et al. [7]. However, there was no measureable change in HIF-1α in this study. Much like with β-catenin, the difference between studies may be related to the lower dose of DFO used in this study, or the different time intervals between final DFO administration and euthanasia. Another more direct mechanism for the decrease in oxidation is through the direct binding of DFO to unbound iron, which leads to a decrease in Fenton chemistry and less oxidative damage [24].

Both soluble and insoluble amyloid levels were drastically increased in the brains of TG mice, but the increase of soluble Aβ40 and Aβ42 was attenuated in DFO-treated mice. An effect of IN DFO on the amyloid cascade in an amyloid model was also seen by Guo et al. [25], which is encouraging, though the sample sizes in that study were small. The lack of a change in plaques is consistent with the results in Hanson et al. [8]. The mechanism of how the amyloid was affected by DFO is unknown, but was suggested to reduce expression and phosphorylation of APP in Guo et al. [25]. Another option is the decrease in protein oxidation, which has been suggested to play an important role in AD [26]. The mechanism could also be related to the decrease in GSK activity [14]. The increase in amyloid in the model also came with an increase in GFAP, which was also seen in amyloid models in Kamphuis et al. [13]. The DFO treatment, however, did not affect the levels of GFAP. Also, though it is not present in the APP/PS1 mouse model, translation of APP mRNA in humans is regulated through an iron response element, which could be affected by removal of iron by DFO.

These data demonstrate that low doses of IN DFO can modify several targets along the multiple pathways implicated in the neuropathology of Alzheimer's making it an attractive candidate for the treatment of this heterogeneous disease. Because IN DFO is beneficial in several animal models of neurodegenerative disease, as well as other brain illnesses, it seems to be functioning via a pleiotropic effect.

Conflict of interest

William H. Frey, 2nd and Leah R. Hanson are inventors on a patent owned by Health Partners Institute for Education and Research regarding the use of intranasal deferoxamine.

Acknowledgments

Thanks to Amanda Cagan, Katherine Faltesek, and Aleta Svitak for help with intranasal dosing and behavior tests. Funded by the Department of Neurosciences Research at HealthPartners Institute for Education and Research.

References

[1] S.D. Skaper, Alzheimer's disease and amyloid: culprit or coincidence? Int. Rev. Neurobiol. 102 (2012) 277–316.
[2] C. Gao, et al., New animal models of Alzheimer's disease that display insulin desensitization in the brain, Rev. Neurosci. 24 (6) (2013) 607–615.
[3] E.P. Raven, et al., Increased iron levels and decreased tissue integrity in hippocampus of Alzheimer's disease detected in vivo with magnetic resonance imaging, J. Alzheimer's Dis. (2013).
[4] S. Ayton, P. Lei, A.I. Bush, Metallostasis in Alzheimer's disease, Free Radical Biol. Med. 62 (2013) 76–89.
[5] M.N. de Lima, et al., Reversion of age-related recognition memory impairment by iron chelation in rats, Neurobiol. Aging 29 (7) (2008) 1052–1059.
[6] D.R. Crapper McLachlan, et al., Intramuscular desferrioxamine in patients with Alzheimer's disease, Lancet 337 (8753) (1991) 1304–1308.
[7] J.M. Fine, et al., Intranasal deferoxamine improves performance in radial arm water maze: stabilizes HIF-1alpha, and phosphorylates GSK3beta in P301L tau transgenic mice, Exp. Brain Res. 219 (3) (2012) 381–390.
[8] L. Hanson, et al., Intranasal delivery of deferoxamine reduces spatial memory loss in APP/PS1 mice, Drug Delivery Transl. Res. (2012) 1–9.
[9] F. Febbraro, et al., Chronic intranasal deferoxamine ameliorates motor defects and pathology in the alpha-synuclein rAAV Parkinson's model, Exp. Neurol. 247C (2013) 45–58.
[10] J.M. Fine, et al., Intranasally-administered deferoxamine mitigates toxicity of 6-OHDA in a rat model of Parkinson's disease, Brain Res. 1574 (2014) 96–104.
[11] G.W. Arendash, et al., Multi-metric behavioral comparison of APPsw and P301L models for Alzheimer's disease: linkage of poorer cognitive performance to tau pathology in forebrain, Brain Res. 1–2 (2004) 29–41, 1012.
[12] L.R. Hanson, et al., Intranasal administration of CNS therapeutics to awake mice, J. Visualized Exp. 74 (2013).
[13] W.et al. Kamphuis, GFAP isoforms in adult mouse brain with a focus on neurogenic astrocytes and reactive astrogliosis in mouse models of Alzheimer disease, PLoS One 7 (8) (2012) e42823.
[14] Z. Cai, Y. Zhao, B. Zhao, Roles of glycogen synthase kinase 3 in Alzheimer's disease, Curr. Alzheimer Res. 9 (7) (2012) 864–879.
[15] A. Petit-Paitel, GSK-3beta: a central kinase for neurodegenerative diseases? Med. Sci. 26 (5) (2010) 516–521 (Paris).
[16] S. Kapoor, Deferoxamine: emerging, new neuro-protective benefits, Neurol. Sci. 34 (2) (2013) 562–575.
[17] S.Y. Aghdam, S.W. Barger, Glycogen synthase kinase-3 in neurodegeneration and neuroprotection: lessons from lithium, Curr. Alzheimer Res. 4 (1) (2007) 21–31.
[18] X. Zhu, et al., Causes of oxidative stress in Alzheimer disease, Cell. Mol. Life Sci. 64 (17) (2007) 2202–2210.
[19] D. Del Rio, A.J. Stewart, N. Pellegrini, A review of recent studies on malondialdehyde as toxic molecule and biological marker of oxidative stress, Nutr. Metab. Cardiovasc. Dis. 15 (4) (2005) 316–328.
[20] H. Bariskaner, et al., Effects of deferoxamine on tissue lactate and malondialdehyde levels in cerebral ischemia, Methods Findings Exp. Clin. Pharmacol. 25 (5) (2003) 371–376.
[21] C. Dinc, et al., Comparison of deferoxamine and methylprednisolone: protective effect of pharmacological agents on lipid peroxidation in spinal cord injury in rats, Spine (Phila Pa 1976) 38 (26) (2013) E1649–E1655.
[22] C.O. Arent, et al., Synergist effects of *n*-acetylcysteine and deferoxamine treatment on behavioral and oxidative parameters induced by chronic mild stress in rats, Neurochem. Int. 61 (7) (2012) 1072–1080.
[23] A.M. Tonin, et al., Long-chain 3-hydroxy fatty acids accumulating in LCHAD and MTP deficiencies induce oxidative stress in rat brain, Neurochem. Int. 56 (8) (2010) 930–936.
[24] J.L. Domingo, Aluminum and other metals in Alzheimer's disease: a review of potential therapy with chelating agents, J. Alzheimer's Dis. 10 (2-3) (2006) 331–341.
[25] C. Guo, et al., Intranasal deferoxamine reverses iron-induced memory deficits and inhibits amyloidogenic APP processing in a transgenic mouse model of Alzheimer's disease, Neurobiol. Aging 34 (2) (2012) 562–575.
[26] A. Eckert, K. Schmitt, J. Gotz, Mitochondrial dysfunction – the beginning of the end in Alzheimer's disease? Separate and synergistic modes of tau and amyloid-beta toxicity, Alzheimer's Res. Ther. 3 (2) (2011) 15.